This article has been accepted for publication in a future issue of this journal, but has not been fully edited. Content may change prior to final publication. Citation information: DOI 10.1109/TIA.2020.2980731, IEEE Transactions on Industry Applications

Energy Management of Islanded Nanogrids through Nonlinear Optimization using Stochastic Dynamic Programming†

Andres Salazar, *Member, IEEE,* Alberto Berzoy, *Member, IEEE,* Wenzhan Song, *Member, IEEE,* and Javad Mohammadpour Velni, *Member, IEEE.*

***Abstract*—Islanded nanogrids (NGs) are autonomous systems consisting of small-scale generation units including renewable energy sources and traditional fuel generators and energy storage systems (ESS) that typically serve few buildings or loads. This work aims at developing and validating a new optimal energy management (EM) algorithm for an islanded NG. To minimize the generator's operating cost and maximize battery availability at each operating cycle, dynamic programming (DP) framework is employed to solve the underlying optimization problem. The goal of the proposed approach is to ensure the use of maximum available solar power and to achieve optimal battery state of charge (SOC). To meet that goal, the management of the ESS is formulated as a stochastic optimal control problem, where nonlinearities in the battery discharging process are considered. A Markov model is constructed for predicting the probability distribution of the solar production used in the stochastic DP formulation. Simulation results are given to illustrate the efficacy of the proposed DP-based approach compared to a rule-based algorithm. Finally, a hardware-in-the-loop system is used to evaluate the real-time operation of the proposed EM algorithm.**

***Index Terms*—Stochastic optimization; Dynamic programming; Time-variant Markov model; Nanogrids.**

I. Introduction

There are several benefits in terms of financial, environmental and security aspects that motivate the installation of renewable energy sources (RESs). Distributed energy resources (DERs) and energy storage systems (ESSs), at the level of end users, cannot only shift peak demand and flatten the consumption pattern but also empower the customers with a level of utility independence [1]. The ecosystem of distributed generation is generally divided into two main types, microgrids (MGs) and nanogrids (NGs) [2]. MGs, which constitute various types of large scale DERs and ESS units connected to the mains, can supply power to load demands generally in the order of megawatts. NGs are normally composed of a single type of RES, an ESS and a fuel/gas generator, with or without the capability of connecting to the utility. Residential NGs are typically designed to serve a single building and are suitable for grid-tied and off-grid operation where maximum power levels are not greater than 10 kW. In case of a grid service interruption, the grid-tied inverter stops the power generation and the RES, ESS and/or the fuel generator form an autonomous NG.

Due to the introduction of NGs, smart buildings are expected to be more self-sustaining with respect to their energy needs [3]. The NG's energy management system (EMS) is responsible for maintaining the balance between the power generated and demands during the islanded periods of operation, avoiding the complete discharge of the ESS by charging them with available RES and/or fuel generator energy [4], [5]. EMS optimization in NGs and MGs has particularly gained interest due to the stochastic behavior of RES and loads, especially in residential systems.

Dynamic programming (DP)-based methods have been recently employed in [6], in which authors used a Monte Carlo simulation method to cope with uncertainties of the RES generation, electricity pricing and load demand for a grid-tied MG. In [7], authors developed an adaptive dynamic programming (ADP) algorithm to solve the optimal battery energy management and control problem in smart residential NGs; however, stochasticity was not considered in the latter work. Comparisons between DP and a rule-based scheduling algorithm for photovoltaic (PV)/generator/batteries nanogrids were presented in [8], [9]. In [9], a deterministic approach was considered, while in [8] a semi-Markov model was used to forecast the PV generation. References [8], [9] both assume a linear process model in the DP problem formulation. A multi-stage stochastic programming structure was proposed in [10], where uncertainties in supply, demand and pricing were considered for a grid-tied MG. Stochasticity in the DERs has been studied in [11] by employing ensemble weather forecasts and a robust linear program for optimizing a generator's fuel cost; this structure, however, only considered uncertainty in the data obtained by the forecast models. Markov chains for modeling uncertainty in the RES generation have been used in [12], where a Stochastic Dynamic Programming (SDP) algorithm was proposed to optimize the cost of the electric grid energy consumption in wind powered NGs with ESS. In [12], a linear optimization problem was considered and only simulation results were provided.

SDP has also been used for the energy management of residential nanogrids with electric vehicles (EVs), where several authors have focused on proposing solutions to the underlying optimization problem by considering stochasticity in the behavior of the EV, i.e., mobility patterns and home loads. In [13], stochastic models of plug-in and plug-out behavior,

A. Salazar is with the Research and Development Department, sonnen Inc, Atlanta, GA 30033. e-mail: andres@sonnen-batterie.com.

A. Berzoy is with the Research and Development Department, sonnen Inc, Atlanta, GA 30033. e-mail: A.BerzoyLlerena@sonnen-batterie.com.

J. Mohammadpour Velni and W. Song are with School of Electrical & Computer Engineering, University of Georgia, Athens, GA 30602. e-mail: javadm@uga.edu.

Manuscript received July 15, 2019; revised November 9, 2019; accepted February 25, 2020.

†This work was partially funded by USDA-NIFA-SCRI Award Number #2018-51181-28365, project Lighting Approaches to Maximize Profits.

0093-9994 (c) 2020 IEEE. Personal use is permitted, but republication/redistribution requires IEEE permission. See http://www.ieee.org/publications_standards/publications/rights/index.html for more information.

This article has been accepted for publication in a future issue of this journal, but has not been fully edited. Content may change prior to final publication. Citation information: DOI 10.1109/TIA.2020.2980731, IEEE Transactions on Industry Applications

energy required for transportation, and electricity pricing were used to minimize electric energy charging costs. A more recent study in [14] proposed an SDP-based method for a smart home, where a stochastic model was used for the load demand and for the arrival and departure time of the pluggable electric vehicles (PEVs). A Markov chain was used in [14] to model the PEV plug-state. None of the aforementioned references considered the use of renewable sources (and of course stochasticity in the renewable energy generation). Authors in [15] use an SDP-based optimization method in a residential photovoltaic application, where the stochasticity is only related to the EV trip time. The authors further proposed the use of Neural Networks (NN) to provide a day-ahead forecast for the PV generation. In our case, a simplified stochastic model based on Markov chains is employed in the proposed SDP-based energy management system.

This paper examines the scheduling of an autonomous hybrid (PV and fuel generation) NG. The goal is to supply the demand through optimal scheduling of the NG's available local resources. A stochastic dynamic programming (SDP) optimization problem over a rolling horizon is formulated for real-time control of the battery state of charge (SOC). This paper is based on an early publication in [16]. The contributions of this paper are: (1) developing a simplified time-variant Markov model for the photovoltaic (PV) power generation; (2) proposing a SDP optimization framework for energy management of a hybrid NG in a rolling time horizon, using the Markov model of PV generation; (3) defining a new multi-objective optimization problem to achieve the least cost operation, where the problem is formulated to minimize the generation cost and maximize the availability of energy stored in the battery at the beginning of next operating cycle; (4) formulate a nonlinear optimization problem, where nonlinearities in the discharging process of the batteries are considered; (5) conducting a comparative study between the proposed SDP framework and a rule-based method.

II. Nanogrid Modeling and Control

A. System Description

The residential NG used in this work is illustrated in Fig. 1. The ESS is an integrated solution of a bidirectional inverter and a set of battery modules. The PV system is composed of an arrangement of PV panels and a solar inverter that always operate at maximum power point tracking (MPPT). The fuel-based generator is a typical gas or liquid propane. The EMS inside of the ESS receives information about the PV production and load demand using external power meters. The goal for the EMS is to minimize the generator's fuel consumption. Red arrows indicate the power flow in the system. Models for each component are described as follows.

1) PV Energy Generation Model: The PV output is connected to a dc/ac converter that only operates when an ac voltage is present at its output. The energy produced by a grid-tied PV system, E_{PV}, can be estimated by

$$E_{PV}[k] = (\eta_{pv}\eta_{inv})(A_{PV} I_0[k]), \tag{1}$$

where k is the discrete time index, and the time horizon is divided into N equal intervals. Also, η_{pv} is the PV module efficiency, I_0 is the solar irradiance measured in Watts per square meter ($\mathrm{W/m^2}$), A_{PV} is the effective area, and η_{inv} is the inverter efficiency, which is around 97%.

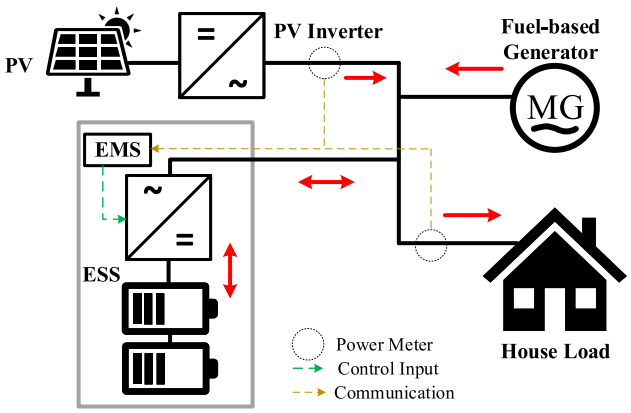

Fig. 1: Configuration of the nanogrid considered in this work.

2) ESS Model: Energy storage systems in residential ac coupled NGs are usually composed of a set of batteries and a bidirectional converter. The energy capacity and density of the system depend on the cells technology. The efficiency in the energy conversion process is generally between 95% and 97% during charging and discharging, respectively. The equations of battery SOC and the energy stored in the battery E_B can be used interchangeably to describe the charging and discharging behavior and the current and future state of ESS operation by the following nonlinear equation

$$SOC[k] = \frac{1}{C_B}\sum_{k=1}^{N}(I_B[k])\Delta t + SOC_0, \tag{2}$$

where I_B is the battery current, which is positive during charging and negative during a discharging period, C_B denotes the battery storage capacity, SOC_0 denotes the initial battery SOC. The energy stored in the battery can be defined by

$$E_B[k+1] = E_B[k] + (P_B[k])\Delta t, \tag{3}$$

where $P_B[k]$ is the charge or discharge power assumed to be constant over the time period between $[k\Delta t, (k+1)\Delta t)$, which is positive during charging and negative during a discharging period. We note that (3) holds true while the battery is charging. However, during discharging period, the process becomes nonlinear following Peukert's effect. According to Peukert's law, the battery discharge time (L_t) can be approximated by

$$L_t = \frac{C_b}{\hat{I}_B}, \tag{4}$$

where

$$\hat{I}_B = (I_{B_{dis}})^{\phi}, \tag{5}$$

with $I_{B_{dis}}$ being the battery current during discharge and $\phi \geq 1$ an exponent which describes the exponential nonlinearity of the discharging process in the battery. If we select the parameter as $\phi = 1$, (4) turns into a linear model which fails to represent the inherent nonlinearity at high discharge currents. The exponential nonlinear relation reveals that higher

0093-9994 (c) 2020 IEEE. Personal use is permitted, but republication/redistribution requires IEEE permission. See http://www.ieee.org/publications_standards/publications/rights/index.html for more information.

This article has been accepted for publication in a future issue of this journal, but has not been fully edited. Content may change prior to final publication. Citation information: DOI 10.1109/TIA.2020.2980731, IEEE Transactions on Industry Applications

discharge currents lead to an exponentially smaller effective capacity [17]. For a real battery, the exponent ϕ is greater than unity. For a lead–acid battery, ϕ is typically between 1.1 and 1.3, whereas for a lithium-ion battery, this constant can vary from 1 to 1.09 [18]. The effect can be also translated into the battery power discharge and define a nonlinear term for the energy stored in the battery based on (3) as

$$E_B[k+1] = E_B[k] + (\hat{P}_B[k])\Delta t. \tag{6}$$

Let us define the battery discharge power as:

$$\hat{P}_B = V_B \hat{I}_B, \tag{7}$$

$$\hat{P}_B = V_B (I_{B_{dis}})^{\phi}, \tag{8}$$

$$P_{B_{dis}} = V_B I_{B_{dis}}, \tag{9}$$

$$\hat{P}_B = V_B (\frac{P_{B_{dis}}}{V_B})^{\phi}. \tag{10}$$

For a Lithium-ion battery, it can be assumed that the battery voltage is constant inside the linear operation region. Therefore

$$\hat{P}_B \approx \alpha_v (P_{B_{dis}})^{\phi}, \tag{11}$$

where α_v is a constant that could vary from 0.5 to 0.7 for nominal battery voltage between 50V and 400V, which is typically acceptable for commercially available battery storage systems. Then, the nonlinear model for the energy stored in the battery is given by

$$E_B[k+1] = \begin{cases} E_B[k] + \alpha_v (P_B[k])^{\phi} \Delta t, & \forall P_B < 0 \\ E_B[k] + (P_B[k])\Delta t, & \forall P_B \geq 0 \end{cases} \tag{12}$$

Constraints imposed on the NG by ESS are given by

$$E_B^{\min} \leq E_B[k] \leq E_B^{\max}, \tag{13}$$

$$E_B^{\min} \leq E_B[k+1] \leq E_B^{\max}, \tag{14}$$

$$-P_{B-\text{discharge}}^{\max} \leq P_B[k] \leq P_{B-\text{charge}}^{\max}. \tag{15}$$

Constraints (13) and (14) impose allowable SOC limits while (15) enforces charging and discharging power limits.

3) Demand Model: Using historic energy consumption data, behavior of the load (E_L) can be forecast. The load in residential applications is seasonal and depends on different factors such as weather, resident standard power usage habit, household size, number of electrical appliances and usage. Generally, autoregressive moving average (ARMA) models have been used to forecast the load [19]. In this work, the load (hourly data) forecast is based on a typical household usage in Atlanta, GA.

4) Generator Model: A gas generator with the following quadratic cost function is considered [20]:

$$C_k(E_G[k]) = \alpha_1 E_G^2[k] + \alpha_2 E_G[k] + \alpha_3, \tag{16}$$

where E_G is the energy generated, and α_1, α_2 and α_3 are coefficients obtained from generator's power curve vs. the amount of fuel consumed. The constraint imposed on the NG by generator is defined by the generator maximum and minimum power limits as

$$P_G^{\min} \leq P_G[k] \leq P_G^{\max}. \tag{17}$$

Another constraint imposed on the NG comes from the power balance, where the generated energy (sum of PV and gas generator) must be equal to the consumed energy (sum of load and the battery energy discharged). The generator energy required for cost calculations is then

$$E_G[k] = E_L[k] + P_B[k]\Delta t - E_{PV}[k] \geq 0, \tag{18}$$

where $P_B[k]$ can be positive or negative, where negative power corresponds to battery discharge.

B. NG's General EMS Operating Rules

A classical approach to the energy management (EM) on off-grid NGs is based on a rule-based heuristic method, in which the PV generated power is considered to be deterministic and the actual values of PV generation and SOC are utilized to determine the control policy for charging or discharging the batteries. The control policy determines the relation between P_B as the control input and E_B as the system state. A rule-based EM algorithm of the NG under consideration is shown in Algorithm 1. Note that whenever the SOC reaches a predefined minimum level (SOC^{min}), the controller starts charging the battery at a fixed, predetermined power, $P_{B_{\text{fixed}}}$, which is generally set to a low value to minimize the fuel consumption. This algorithm is executed every time step after the battery charging /discharging process occurs.

Algorithm 1 Rule-based EM algorithm

procedure GENERATOR OFF
  if $SOC[k] > SOC^{\min}$ & $SOC[k] < SOC^{\max}$ **then**
    $P_B[k] = P_{PV}[k] - P_L[k]$
  if $SOC[k] \geq SOC^{\max}$ **then**
    $P_B[k] = -P_L[k]$
  $P_G[k] \leftarrow 0$
  if $SOC[k] = SOC^{\min}$ **then**
    goto **procedure** GENERATOR ON.
procedure GENERATOR ON
  $P_B[k] = P_{B_{\text{fixed}}}$
  $P_G[k] \leftarrow P_L[k] + P_B[k]$
  if $SOC[k] = SOC^{\max}$ **then**
    goto **procedure** GENERATOR OFF.

III. NANOGRID OPTIMAL ENERGY MANAGEMENT

A. Formulation of Nonlinear Optimization Problem

To achieve an optimal EM, the generation cost (16) has to be minimized by finding the battery charging schedule $P_B[k]$ while satisfying power balance equation and all aforementioned operational constraints over the entire operating time horizon T. The EM problem is formulated as a finite horizon constrained quadratic problem. However, the computational complexity increases exponentially with T. Also, in practice, accurate values of inputs (e.g., load profile and PV power)

0093-9994 (c) 2020 IEEE. Personal use is permitted, but republication/redistribution requires IEEE permission. See http://www.ieee.org/publications_standards/publications/rights/index.html for more information.

This article has been accepted for publication in a future issue of this journal, but has not been fully edited. Content may change prior to final publication. Citation information: DOI 10.1109/TIA.2020.2980731, IEEE Transactions on Industry Applications

are not available for the whole operating horizon in advance. Therefore, the solution to the original finite time horizon problem can be approximated with that of the corresponding receding time horizon (RTH) optimization problem. To ensure a continuous optimal operation, an additional optimization objective is added to the performance index function J, which is the terminal cost to avoid depleting battery at the end of the optimization horizon. The battery optimal scheduling for k^{th} time step (for any $k \in \{0, ..., N-1\}$) can be represented by

$$\begin{aligned} \min_{P_B[k]} \quad & J = \sum_{k=k_0}^{k_f-1} C_k(E_G[k]) + \gamma(E_B^{\max} - E_B[k_f]), \\ \text{s.t.} \quad & E_B[k+1] = \begin{cases} E_B[k] + \alpha_v (P_B[k])^{\phi} \Delta t, & \forall P_B < 0 \\ E_B[k] + (P_B[k]) \Delta t, & \forall P_B \geq 0 \end{cases} \\ & E_B^{\min} \leq E_B[k] \leq E_B^{\max}, \\ & E_G^{\min} \leq E_G[k] \leq E_G^{\max}, \\ & P_B^{\min} \leq P_B[k] \leq P_B^{\max}, \\ & E_G[k] \geq 0, \end{aligned} \tag{19}$$

where k_0 is the current time step, $k_f = N + k_0 - 1$ and γ is a weight factor. The above optimization problem is solved at every time step with updated inputs, and the first battery charge/discharge (control action) is implemented as the optimal control policy. More details about the RTH optimization and its applications in EMS can be found in [21] and [22]. It is noted that the above optimization problem is nonlinear due to the battery dynamics appeared in the constraints.

B. Stochastic Optimal Energy Management

In practice, power output shows stochasticity due to unpredictable behavior of solar and weather variations. The PV generated power is first modeled as a time-variant Markov process, and then the optimal EM problem is formulated as an RTH quadratic program and solved using SDP.

A.1: PV Power Density Forecast using Markov Models

First-step Discrete-time Markov Model: This is a probabilistic model, in which the transitions from one state to another are directed by discrete probabilities obtained from the statistics of real historical data. The transition matrix (TM) $\boldsymbol{M} = [m_{\epsilon\lambda}] \in \mathbb{R}^{n \times n}$ serves as a probability model that describes the transitions between states on the finite state space $S = \{s_1, ..., s_n\}$, and whose entries are defined as

$$m_{\epsilon\lambda} = \text{Prob}(E_{PV_{k+1}} = s_\lambda | E_{PV_k} = s_\epsilon), \tag{20}$$

where s_ϵ is the state of $E_{PV_k} = E_{PV}[k]$ at the time instant k and s_λ is the state of $E_{PV_{k+1}}$ at $(k+1)^{\text{th}}$ time instant. A TM with rows $\boldsymbol{m}_1, .., \boldsymbol{m}_n$ meets the following properties [23]:

$$\begin{cases} \sum_{\lambda=1}^{n} m_{\epsilon\lambda} = 1 & \forall \epsilon \in \{1, ..., n\}, \\ m_{\epsilon\lambda} \geq 0, & \forall \epsilon, \lambda \in \{1, ..., n\}. \end{cases} \tag{21}$$

The probability that after the k^{th} transition, the state is $x_k = s_\lambda$, given that the initial state is $E_{PV_0} = s_\epsilon$, is defined by

$$\text{Prob}(E_{PV_k} = s_\lambda | E_{PV_0} = s_\epsilon) = m_{\epsilon\lambda}^k, \tag{22}$$

where there is a time-variant Markov model with one TM for each time instant.

Let π_k^ϵ be the probability distribution of E_{PV_k} such that

$$\pi_k^\epsilon = \text{Prob}(E_{PV_k} = s_\epsilon). \tag{23}$$

In a Markov process, an initial probability distribution can be propagated in time. Then, the propagation of the distribution for future time instants is given by

$$\pi_k = \sum_{\epsilon=1}^{n} (\pi_0^\epsilon \prod_{k=1}^{N} \boldsymbol{M_k}), \tag{24}$$

where $\boldsymbol{M_k}$ is the TM of the k^{th} time instant state transition.

Markov Chain for Predicting Hourly Solar Radiation: Markov properties of the solar radiation have been studied in [24]. Here, a discrete time-variant Markov model is used for estimating the hourly clear index and generating the daily shape of solar radiation on a monthly basis. The proposed Markov model is a simplified version of that in [25]. We leverage the nature of solar radiation (i.e., an average rising behavior in the morning, an average falling behavior in the afternoon, and a smooth behavior around noon) to extract a time-variant TM for estimating the radiation in transition between states for a 24-hour time horizon ($N = 24$). The simplified Markov model proposed here obtains the daily probability distribution of the radiation by dividing the day into four different time zones, one for the sun rising (zone T_1), one for the mid day (zone T_2), one for the sun falling (zone T_3), and finally one for the absence of sun (zone T_0). This is depicted in Fig. 2. For zone T_0, the TM $\boldsymbol{M}_{T_0} = 0_{n,n}$ is used. Due to a zero or a very low level of solar energy for this zone, a null power generation is assumed. The zones T_1, T_2 and T_3 are respectively denoted by the TMs $\boldsymbol{M}_{T_1}$, $\boldsymbol{M}_{T_2}$ and $\boldsymbol{M}_{T_3}$. The TM of each zone is determined separately using the historical data related to that part of the day assumed to be independent of the TMs of other zones. This results in radiation transitions that may not infringe the statistics of other transition frequencies.

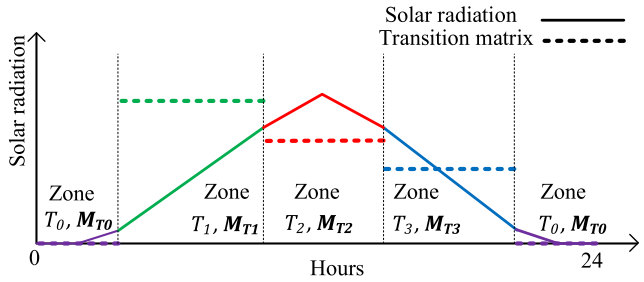

Fig. 2: Four zones of operation considered in obtaining the probability distribution of daily solar radiation.

In order to obtain the TM for the solar energy generation, the generated energy (Wh/m^2) is discretized in n states each

0093-9994 (c) 2020 IEEE. Personal use is permitted, but republication/redistribution requires IEEE permission. See http://www.ieee.org/publications_standards/publications/rights/index.html for more information.

This article has been accepted for publication in a future issue of this journal, but has not been fully edited. Content may change prior to final publication. Citation information: DOI 10.1109/TIA.2020.2980731, IEEE Transactions on Industry Applications

representing a region of occurrence, i.e.,

$$\begin{aligned} s_1: \quad & 0 \le E_{PV}[k] \le \frac{E_{PV}^{\max}}{n}, \\ & \vdots \\ s_n: \quad & \frac{(n-1)\times E_{PV}^{\max}}{n} < E_{PV}[k] \le E_{PV}^{\max}, \end{aligned} \tag{25}$$

where $E_{PV}^{\max}$ is the maximum hourly radiation level, and the number of states, n, is determined based on $E_{PV}^{\max}$.

From a set of historical hourly solar radiation data in one month, the frequency of transitions from state ϵ to λ, $f_{\epsilon,\lambda}$, is found. Subsequently, the frequencies are converted into probabilities

$$m_{\epsilon\lambda} = \frac{f_{\epsilon,\lambda}}{N_{f_{\epsilon,\lambda}}}, \tag{26}$$

where $N_{f_{\epsilon,\lambda}}$ is the total transitions. At each time zone T_l, where $l \in \{0,1,2,3\}$, the same procedure is employed to determine TM.

A.2: Optimal Energy Management using SDP

In this section, the proposed time-variant Markov model for PV prediction is employed in NG's EM problem formulated as a stochastic time-varying optimal control problem. Using the proposed stochastic EM approach, expected cost of NG operation is minimized over the operating horizon. The stationary TMs are described as before.

Using the Markov model of the PV generation, considering the battery energy and PV generation as the system states, i.e., $\mathbf{x_k} = [x_1, x_2]^T = [E_B, E_{PV}]^T$, and by assuming $\mathbf{u_k} = [u_1] = [P_B]$ as the input vector and $\mathbf{d_k} = [d_1] = [E_L]$ as the load vector, the NG state-space model becomes:

$$\mathbf{x_{k+1}} = \begin{cases} \begin{bmatrix} x_1[k+1] \\ x_2[k+1] \end{bmatrix} = \begin{bmatrix} x_1[k] + (u_1[k])^{\phi}\Delta t \\ h_k(x_2[k], w_k) \end{bmatrix}, & \forall u_1[k] < 0 \\ \begin{bmatrix} x_1[k+1] \\ x_2[k+1] \end{bmatrix} = \begin{bmatrix} x_1[k] + (u_1[k])\Delta t \\ h_k(x_2[k], w_k) \end{bmatrix}, & \forall u_1[k] \ge 0 \end{cases} \tag{27}$$

where w_k is a random variable with independent samples and h_k is the probability density that satisfies

$$\text{Prob}\{h_k(s_i, w_k = s_j)\} = m_{ij}^k. \tag{28}$$

To minimize the NG operational cost, sum of the gas generator cost over the optimization horizon should be minimized; therefore, we consider the generation cost at time step k as the stage cost g_k defined by

$$g_k = C_k\big(-x_2[k] + d_1[k] + u_1[k]\Delta t\big). \tag{29}$$

Furthermore, the terminal cost g_N is considered as

$$g_N = \omega_1(E_B^{\max} - x_1[N]), \tag{30}$$

where ω_1 is a weight on terminal cost. The terminal cost enforces battery to stay sufficiently charged. With the stage cost g_k as the fuel generator cost, the expected performance index function J_s becomes $J_s = \mathbf{E}\big(\sum_{k=0}^{N-1} g_k + g_N\big)$, in which $\mathbf{E}(\cdot)$ denotes the expected value of the associated random process. To minimize the NG operational cost, the expected performance index function has to be minimized over the control input u_2 subject to state-space equations (27) and physical constraints represented by (19). By applying Bellman operator, the stochastic optimization problem is divided into a recursive single step optimization

$$\mu_k^*(\mathbf{x_k}) = \underset{u_{1_k}}{\arg\min}(\mathbf{E_{gf}}) \tag{31a}$$
$$\mathbf{E_{gf}} = \mathbf{E}\big(g_k\big) + \mathbf{E}\big(V_{k+1}^*(\mathbf{x_{k+1}})\big)$$

$$V_k^*(\mathbf{x_k}) = \mathbf{E}\big(g_k\big) + \mathbf{E}\big(V_{k+1}^*(\mathbf{x_{k+1}})\big). \tag{31b}$$

The above problems need be solved backward in time. By solving the above time-varying SDP, the battery charge/discharge policy is calculated and the first step control input is implemented. Summary of the SDP algorithm is shown in Algorithm 2.

Algorithm 2 Stochastic DP algorithm

procedure FUNCTION ASSIGNMENT
  $g_k \leftarrow C_k(E_G[k])$
  $g_N \leftarrow \omega_1(E_B^{\max} - E_{B_N})$
  $V_N^* := g_N$
  $\mathbf{u_k} = [P_B]$
  $\mathbf{x_k} = [x_1, x_2]^T = [E_B, E_{PV}]^T$
procedure MINIMIZATION
  for $k = N-1:0$ **do**
    Solve (31a) for $\mu_k^*(\mathbf{x_k})$
    Update $V_k^*(\mathbf{x_k})$ using (31b)
  $u_{2_0} \leftarrow \mu_0^*$

A.3: Real-Time SDP Implementation

The practical implementation and programming of the optimization algorithm based on SDP is presented in the flowchart diagram depicted in Fig. 3. Before proceeding with the description of the flowchart, it is worth mentioning that the SDP algorithm needs to have information about the discrete state values and the control input as defined in Algorithm 2. The following definitions are made and corresponding information is fed into the algorithm initially:

$$x_1(\cdot) \in \mathbb{R}^{n_1}, x_2(\cdot) \in \mathbb{R}^{n}, d_1(\cdot) \in \mathbb{R}^{N}, u_1(\cdot) \in \mathbb{R}^{n_2}.$$

$$\mathbf{g_N}(\cdot) : dim[\mathbf{g_N}(\cdot)] = n_1 \times n$$

$$\mathbf{M_{k_t}}(\cdot) : dim[\mathbf{M_{k_t}}(\cdot)] = n \times n$$

The algorithm is initialized at every control decision step (k). The time horizon (N) is assigned to a variable k which is going to keep track of the rolling horizon iteration. For the first iteration, a matrix $\mathbf{J_{togo}}$ is filled with the coefficients corresponding to the final cost that is desired to be achieved from each one of the initial states. Depending on the current time step in the optimization rolling horizon (k), the transition matrix is copied into a variable $\mathbf{P}$, following the procedure described in section A.1. Three nested loops are used to calculate the cost to go matrix for the current time horizon step (k). A temporary cost vector $J_o \in \mathbb{R}^{n_2}$ is calculated

0093-9994 (c) 2020 IEEE. Personal use is permitted, but republication/redistribution requires IEEE permission. See http://www.ieee.org/publications_standards/publications/rights/index.html for more information.

This article has been accepted for publication in a future issue of this journal, but has not been fully edited. Content may change prior to final publication. Citation information: DOI 10.1109/TIA.2020.2980731, IEEE Transactions on Industry Applications

using (31b). Here the value of the next state for $x_1(k+1)$ is calculated according to (3). This value is then used to obtain the index (idx), which is the argument of the vector x_1 for the calculated value. f is a temporary variable used in the expected value calculation. After all of the discrete values for the input are considered, the minimum cost is stored in the corresponding coefficient for the cost to go matrix and an additional matrix $\mathbf{U}^*$ is used to store the argument or index for which this minimum is achieved. The iterations are completed for all the possible states, and the cost to go matrix is used for the following k_{th} iteration. The beginning of the time horizon is reached, and the current states are checked by assigning their arguments to the variables $idx1$ and $idx2$, which are the indexes to determine optimum value for the input from matrix $\mathbf{U}^*$.

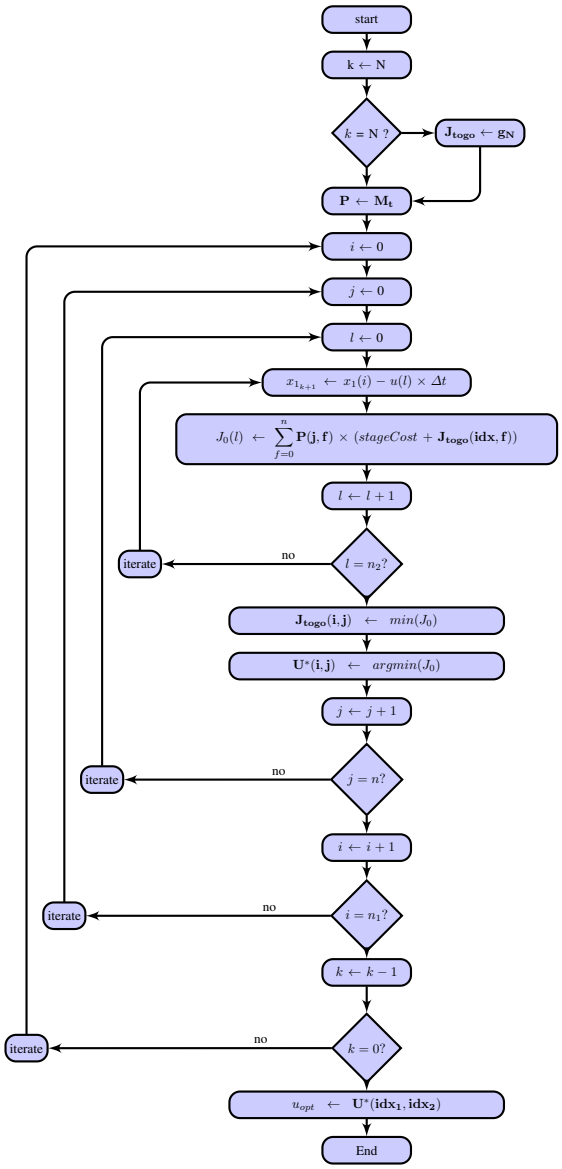

Fig. 3: Flowchart diagram of the SDP algorithm

As an illustrative example, consider the diagram with only few states shown in Fig. 4. An example of the transition probability for the dynamic programming algorithm when $n_1 = 3$ and $n = 3$ is shown. Notice that the two states x_1 and x_2 form a 3×3 matrix with all the states options on the time step k. The transition between states would have as many options as admissible inputs are allowed by the transition probability matrix; however, the total case of transitions could vary depending on the system behavior. For this example, all the transitions are possible which give 9 per state, in total would be as many as 81 possible transitions (not drawn in Fig. 4). In the figure, the 9 cases of transitions for the state $[x_1(i = 2), x_2(j = 2)]$ are defined by the arrows, and two of them are specified. If the system is in the state $[x_1(i = 2), x_2(j = 2)]$, then PV probability distribution is defined as $\text{Prob}(s_{22} \to s_{02}) = m_{22\to02}$ which indicates the probability that the system will be in the state $[x_1(i = 2), x_2(j = 0)]$ at the next discrete time $k + 1$ moment.

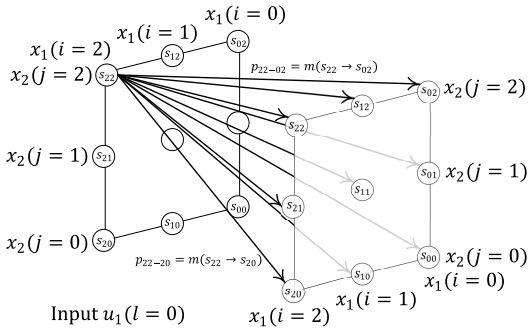

Fig. 4: An illustrative example for $n_1 = 3$ and $n = 3$ at $l = 0$. Transition probability diagram for different values of the PV is shown here.

IV. Simulation and HIL Test Results

For the purpose of verification and comparison of the proposed optimal EM algorithm, simulation and real-time hardware-in-the-loop (HIL) tests are performed in MATLAB/Simulink environment and OPAL RT, respectively. The main parameters of the NG (as shown in Fig. 1) are given in Table I. The parameters are chosen based on an available commercial prototype for residential applications. Simulations

TABLE I: Nanogrid parameters

Parameter	Value	Parameter	Value
E_B^{max}	$6k$Wh	ω_1	7×10^8
E_B^{min}	300Wh	I_0^{max}	$1.018\frac{\text{kWh}}{\text{m}^2}$
$P_{B-charge}^{max}$	$4k$W	η_{pv}	0.19
$P_{B-discharge}^{max}$	$3.5k$W	η_{inv}	0.98
P_G^{max}	$8k$W	A_{PV}	18m^2
P_G^{min}	$0k$W	T	24 hours
P_{PV}^{max}	$5k$W	Δt	1 hour
α_1	1.2898×10^{-9}	N	24
α_2	1.3609×10^{-4}	n	22
α_3	0.9117×10^{-16}	ϕ	1.09
n_1	120	n_2	115
α_v	0.6	G_{price}	$0.5\frac{USD}{thm}$

of the NG energy management start from the same initial

0093-9994 (c) 2020 IEEE. Personal use is permitted, but republication/redistribution requires IEEE permission. See http://www.ieee.org/publications_standards/publications/rights/index.html for more information.

This article has been accepted for publication in a future issue of this journal, but has not been fully edited. Content may change prior to final publication. Citation information: DOI 10.1109/TIA.2020.2980731, IEEE Transactions on Industry Applications

condition, i.e., $E_B(0) = E_B^{\max}$. In addition, the daily PV generation profile is taken from the solar radiation data from *NREL* database [26].

A. Results for the Simulated NG System

1) Evaluation of the Markov Model: In order to validate the proposed model, 15-year solar radiation data of the month of July of a site located in Elizabeth City, North Carolina, extracted from the *NREL* database is used. The model is learned using 13 years of data and validated on the other two years data. The maximum hourly radiation of the site is $I_0^{max} = 1.018\ k\text{Wh/m}^2$, and the number of Markov model states is considered to be $n = 22$ with the states taking values as $s_i \in \{0, 1, ..., 21\}$ for $\forall i \in \{1, ..., 22\}$.

In order to evaluate the performance of the proposed time-variant Markov model, data from the average day of the two years is selected. The results of the Markov model for each hour have a probability distribution; the expected value of each probability distribution is used for the evaluation of the results. The PV output predicted by the proposed model for the subsequent 24 hours is compared with the time-invariant Markov model and the real data in Fig. 5. As observed, the model is able to follow the real mean profile, while closely approximating the standard deviation for the obtained data. In order to show the improvements achieved by the proposed model compared to the time-invariant model, the relative root mean square error ($RRMSE$) is used to quantify the total estimation error.

$RRMSE$ value achieved by the proposed model is 9.14%, whereas the error with the stationary (time-invariant) model is 31.3%. Using the proposed model, *the error considerably decreases while the computational complexity nearly remains the same*. Next, simulation results using SDP are compared

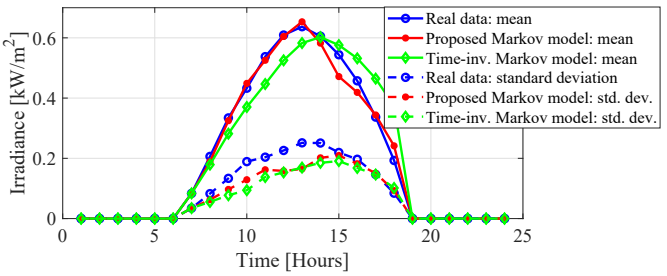

Fig. 5: Comparison of hourly mean and standard deviation between proposed time-variant Markov model and the real data.

against those obtained from the rule-based algorithm.

2) Comparative Assessment of Rule-based EM and SDP-based Approach: Two cases are simulated considering different solar irradiance levels over a period of 72 hours. The first one is shown in Fig. 6, where three consecutive days with good irradiance are presented. The comparison between battery SOC for rule-based ($SOC_{B_{rule}}$) and SDP-based ($SOC_{B_{sdp}}$) methods is shown in the third subplot. Generation power for both algorithms is also shown in this figure. With the SDP approach, the EMS is able to consume less generator power over the three days and finish each day with a higher battery SOC index. The rule-based algorithm charges the battery whenever the energy stored in the battery is below 2 kWh. On the other hand, the underlying optimization problem for the SDP method is solved on a rolling horizon basis. The prediction horizon is assumed to be 24 hours, and at each hour, it determines the optimal policy for the next 24 hours. The control policy for this case is the battery charge/discharge power (control input) as a function of battery stored energy and PV generated energy (which are the system states). Table II shows the cost of operating the generator each day and the availability index in Wh, which is the battery SOC at the end of each day. Results showed that after the third day of operation, the user could save up to 20% of the generator's cost if the SDP method is employed. Fig. 7 shows the system behavior assuming that the second day irradiance is proportionally lower than the other two days. In this case, the total saving for operating the NG could be up to 7% if the SDP algorithm is used.

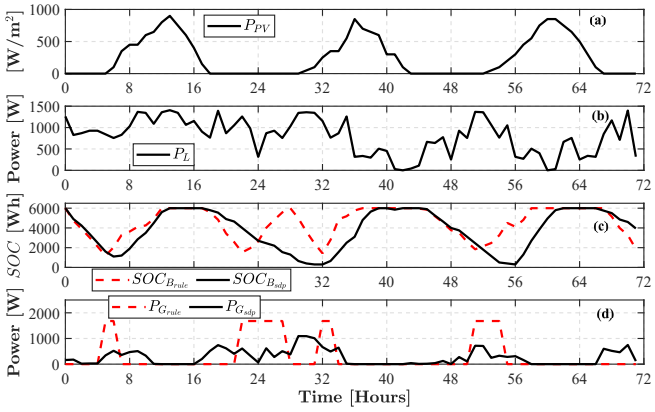

Fig. 6: Simulation results for three consecutive days with good irradiance levels. (a) P_{PV} (PV available power), (b) P_L (load power), (c) battery SOC, and (d) P_G (fuel generator power).

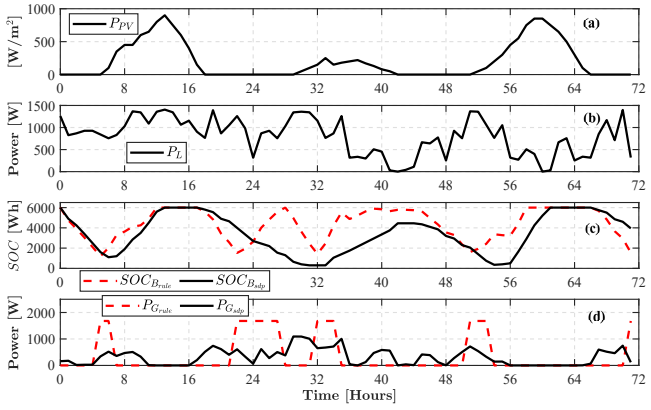

Fig. 7: Simulation results for three consecutive days, assuming that the second day has a lower irradiance level. (a) P_{PV} (PV available power), (b) P_L (load power), (c) battery SOC, and (d) P_G (fuel generator power).

0093-9994 (c) 2020 IEEE. Personal use is permitted, but republication/redistribution requires IEEE permission. See http://www.ieee.org/publications_standards/publications/rights/index.html for more information.

This article has been accepted for publication in a future issue of this journal, but has not been fully edited. Content may change prior to final publication. Citation information: DOI 10.1109/TIA.2020.2980731, IEEE Transactions on Industry Applications

B. Real-time HIL Simulation Results

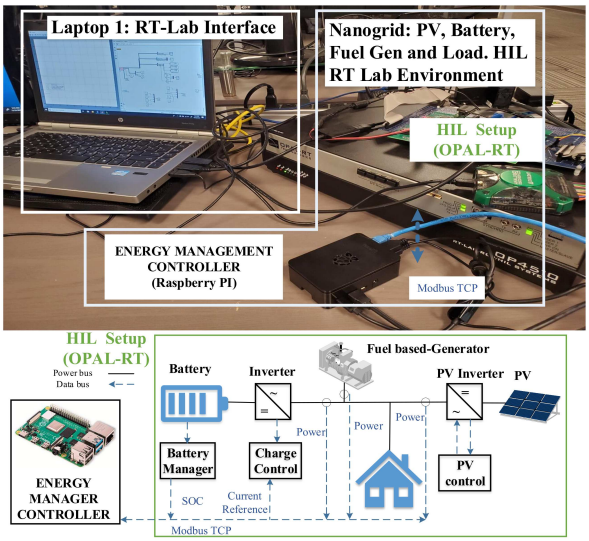

Fig. 8: Setup for the real-time Hardware-in-the-Loop

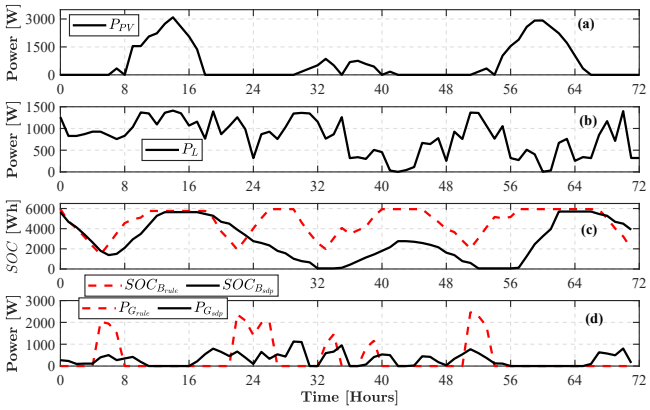

Fig. 9: HIL results of 72 hours. (a) P_{PV} (PV available power), (b) P_L (load power), (c) battery SOC, and (d) P_G (fuel generator power).

Performance of the two proposed methods (rule-based and SDP) is evaluated using OPAL-RT Model-In-the-Loop real-time experiments. The NG is implemented in the OPAL-RT unit using dynamic models for the inverters, batteries, PV panels and generator. The interface RT-lab is executed in Laptop 1 of Fig. 8. The EMS is developed in Python and implemented in a $RaspberyPi4$ which receives the measurement data and sends the control input via Modbus TCP/IP. An overview of the experimental platform is shown in the bottom half of Fig. 8. The HIL simulation results of the generated power, consumption and the battery energy for the two proposed energy management algorithms are illustrated in Fig. 9 for a period of 72 hour. During this experiment, nonlinear SDP algorithm uses a ϕ value of 1.09. At the end of the first day, the SDP method exhibits better Battery Availability Index than the rule-based method; however, in the second day, it fails in obtaining a superior index than the rule-based method. The situation is over ruled by the third day when the SDP implementation is able to show better performance. In general, the total generator operating cost (for generator fuel consumption) using the rule-based approach was *US*$3.5537, whereas the total cost for the generator usage under the SDP-based method was *US*$2.8493, representing a saving of 19%.

TABLE II: Three days performance comparison using rule-based and stochastic DP methods.

Generator fuel cost ($/day)			Battery availability index (Wh)	
Day	Rule-based	SDP	Rule-based	SDP
1	0.9291	0.8705	1,944	3,350
2	1.3936	0.9713	4,650	4,650
3	0.9291	0.7638	1,872	3,950

V. Conclusions

Two algorithms were devised in this paper aiming at scheduling the battery charge and discharge in an NG supplied by both traditional and renewable sources while considering operational constraints to yield maximum financial and operational benefits. SDP was employed to achieve an optimal EM, in which a nonlinear optimization problem was formulated over a finite number of stages and on a rolling horizon basis. The use of a time-variant Markov model was also proposed in this paper. The simulation and HIL results confirmed that the stochastic EM strategy was able to effectively cope with the economical requirements much better than the rule-based approach in an autonomous mode. Furthermore, the stochastic approach could also cope with modeling and capturing uncertainties in PV generation. The SDP-based approach guaranteed the minimum operating cost by minimizing the fuel generator operating times during each cycle, and simultaneously improving the availability of battery in the next cycle by elevating its SOC at the end of each cycle.

VI. Acknowledgments

The authors thank Mr. Farid Khazali for his contribution in the early stage of this work.

References

[1] R. P. S. Chandrasena, F. Shahnia, S. Rajakaruna, and A. Ghosh, "Dynamic operation and control of a hybrid nanogrid system for future community houses," *IET Generation, Transmission Distribution*, vol. 9, no. 11, pp. 1168–1178, 2015.

[2] A. Werth, N. Kitamura, and K. Tanaka, "Conceptual study for open energy systems: Distributed energy network using interconnected DC nanogrids," *IEEE Transactions on Smart Grid*, vol. 6, no. 4, pp. 1621–1630, July 2015.

[3] N. Kumar, A. V. Vasilakos, and J. J. P. C. Rodrigues, "A multi-tenant cloud-based DC nanogrid for self-sustained smart buildings in smart cities," *IEEE Communications Magazine*, vol. 55, no. 3, pp. 14–21, March 2017.

[4] N. Liu, X. Yu, W. Fan, C. Hu, T. Rui, Q. Chen, and J. Zhang, "Online energy sharing for nanogrid clusters: A lyapunov optimization approach," *IEEE Transactions on Smart Grid*, vol. 9, no. 5, pp. 4624–4636, Sep. 2018.

0093-9994 (c) 2020 IEEE. Personal use is permitted, but republication/redistribution requires IEEE permission. See http://www.ieee.org/publications_standards/publications/rights/index.html for more information.

This article has been accepted for publication in a future issue of this journal, but has not been fully edited. Content may change prior to final publication. Citation information: DOI 10.1109/TIA.2020.2980731, IEEE Transactions on Industry Applications

[5] S. M. Dawoud, X. Lin, and M. I. Okba, "Hybrid renewable microgrid optimization techniques: A review," *Renewable and Sustainable Energy Reviews*, vol. 82, no. May 2017, pp. 2039–2052, 2018.

[6] H. Shuai, J. Fang, X. Ai, Y. Tang, J. Wen, and H. He, "Stochastic optimization of economic dispatch for microgrid based on approximate dynamic programming," *IEEE Transactions on Smart Grid*, vol. 3053, no. c, pp. 1–13, 2018.

[7] Q. Wei, D. Liu, F. L. Lewis, Y. Liu, and J. Zhang, "Mixed iterative adaptive dynamic programming for optimal battery energy control in smart residential microgrids," *IEEE Transactions on Industrial Electronics*, vol. 64, no. 5, pp. 4110–4120, 2017.

[8] A. K. Barnes, J. C. Balda, and A. Escobar-Mejía, "A semi-markov model for control of energy storage in utility grids and microgrids with pv generation," *IEEE Transactions on Sustainable Energy*, vol. 6, no. 2, pp. 546–556, April 2015.

[9] S. Sheng, P. Li, C. Tsu, and B. Lehman, "Optimal power flow management in a photovoltaic nanogrid with batteries," in *2015 IEEE Energy Conversion Congress and Exposition (ECCE)*, Sep. 2015, pp. 4222–4228.

[10] A. Bhattacharya, J. P. Kharoufeh, and B. Zeng, "Managing energy storage in microgrids: A multistage stochastic programming approach," *IEEE Transactions on Smart Grid*, vol. 9, no. 1, pp. 483–496, 2018.

[11] E. Craparo, M. Karatas, and D. I. Singham, "A robust optimization approach to hybrid microgrid operation using ensemble weather forecasts," *Applied Energy*, vol. 201, no. 5, pp. 135–147, 2017.

[12] A. Belloni, L. Piroddi, and M. Prandini, "A stochastic optimal control solution to the energy management of a microgrid with storage and renewables," *Proceedings of the American Control Conference*, vol. 2016-July, pp. 2340–2345, 2016.

[13] J. Donadee and M. D. Ilić, "Stochastic optimization of grid to vehicle frequency regulation capacity bids," *IEEE Transactions on Smart Grid*, vol. 5, no. 2, pp. 1061–1069, 2014.

[14] X. Wu, X. Hu, X. Yin, and S. J. Moura, "Stochastic optimal energy management of smart home with PEV energy storage," *IEEE Transactions on Smart Grid*, vol. 9, no. 3, pp. 2065–2075, 2018.

[15] X. Wu, X. Hu, S. Moura, X. Yin, and V. Pickert, "Stochastic control of smart home energy management with plug-in electric vehicle battery energy storage and photovoltaic array," *Journal of Power Sources*, vol. 333, no. October, pp. 203–212, 2016.

[16] A. Salazar, A. Berzoy, J. Mohammadpour Velni, and W. Song, "Optimum energy management of islanded nanogrids through nonlinear stochastic dynamic programming," in *2019 IEEE Industry Applications Society Annual Meeting (IAS)*, Sep. 2019, pp. 1–8.

[17] A. S. Akyurek and T. S. Rosing, "Optimal Distributed Nonlinear Battery Control," *IEEE Journal of Emerging and Selected Topics in Power Electronics*, vol. 5, no. 3, pp. 1045–1054, 2017.

[18] N. Omar, M. Daowd, P. Van den Bossche, O. Hegazy, J. Smekens, T. Coosemans, and J. Van Mierlo, "Rechargeable energy storage systems for plug-in hybrid electric vehicles—assessment of electrical characteristics," vol. 5, pp. 2952–2988, 12 2012.

[19] S. S. Pappas, L. Ekonomou, D. C. Karamousantas, G. E. Chatzarakis, S. K. Katsikas, and P. Liatsis, "Electricity demand loads modeling using autoregressive moving average (ARMA) models," *Energy*, vol. 33, no. 9, pp. 1353–1360, 2008.

[20] M. Z. Djurovic, A. Milacic, and M. Krsulja, "A simplified model of quadratic cost function for thermal generators," *Proceedings of the 23rd DAAAM Symposium*, vol. 23, no. 1, pp. 25–25, 2012.

[21] D. P. Bertsekas, *Dynamic programming and optimal control*. Athena scientific Belmont, 2005, vol. 1, no. 3.

[22] M. Rafiee Sandgani and S. Sirouspour, "Energy management in a network of grid-connected microgrids/nanogrids using compromise programming," *IEEE Transactions on Smart Grid*, vol. 9, no. 3, pp. 2180–2191, May 2018.

[23] M. L. Puterman, *Markov decision processes: discrete stochastic dynamic programming*. John Wiley & Sons, 2014.

[24] M. M. P. Poggi, G. Notton and A. Louche, "Stochastic study of hourly total solar radiation in Corsica using a Markov model," *International journal of climatology*, vol. 20, no. 14, pp. 1843–1860, 2000.

[25] V. Chamola and B. Sikdar, "A Multistate Markov Model for Dimensioning Solar Powered Cellular Base Stations," *IEEE Transactions on Sustainable Energy*, vol. 6, no. 4, pp. 1650–1652, 2015.

[26] N. R. E. L. (NREL)., "Monthly data files & reports." [Online]. Available: $http://rredc.nrel.gov/solar/new_data/confrrm/ec/$

Andres Salazar received the BS degree in Electronics Engineering from Universidad del Norte in Colombia and MS degree in Electrical Engineering from University of Puerto Rico. He has been author and coauthor of several publications in the field of Renewable Energy Generation and Energy Storage. Mr Salazar has more than 8 years of industry experience in the development of Grid-tied photo-voltaic Inverters and Energy Storage Systems. He is currently working as the Manager of Power Electronics Development at the R&D department of sonnen Inc (wholly owned subsidiary of Shell within its New Energies division) in Atlanta GA, where he is leading the development of Lithium-Ion Energy Storage systems for residential applications. At the same time he is pursuing a PhD in Electrical Engineering at the University of Georgia. His research interests include nonlinear and optimal control for power converters.

Alberto Berzoy (S'13-M'19) received the B.Sc. and M.Sc. degrees in Electronics Engineering from the Universidad Simon Bolivar, Caracas, Venezuela, in 2003 and 2008, respectively. He received PhD degree from Florida International University (FIU), Miami, USA in 2018. He is currently working as a Power Electronics and Control Engineer at the R&D department of sonnen inc where he is working on the development of last generation of inverters for Energy Storage Systems in residential applications. His seventeen years of research and ten teaching experience include power electronics converter design and control, electrical machines drives, diagnosis and condition monitoring, digital signal processing, model predictive control and digital control systems. Among the research interest areas, Dr. Berzoy is captivated by electric vehicles and renewable energy applications. He has served or currently serves as reviewer of several IEEE Transactions including the IEEE Transactions on Energy Conversion, the IEEE Transactions on Power Electronics, IEEE Transactions on Industry Applications and IEEE Transactions on Magnetics.

Wenzhan Song received the B.S. and M.S. degrees from the Nanjing University of Science and Technology, Nanjing, China, in 1997 and 1999, respectively, and the Ph.D. degree in computer science from the Illinois Institute of Technology, Chicago, IL, USA, in 2005.,He is currently the Chair Professor of Electrical and Computer Engineering with the University of Georgia, Athens, GA, USA. His current research interests include cyber-physical systems and their applications in energy, environment, food, and health sectors.Dr. Song received the National Science Foundation CAREER Award in 2010.

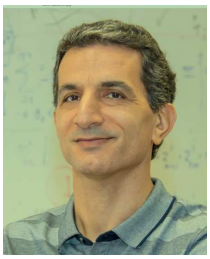

Javad Mohammadpour Velni received BS and MS degrees in electrical engineering from Sharif University of Technology and University of Tehran, Iran, respectively, and PhD degree in mechanical engineering from University of Houston, TX. He is currently an associate professor of electrical engineering at the University of Georgia (UGA), where he joined in 2012. Prior to that, he was with the University of Michigan, where he worked in the naval architecture & marine engineering department from Oct. 2011 to Jul. 2012. He was also a Research Assistant Professor of mechanical engineering at University of Houston from Oct. 2008 to Sep. 2011 and a Research Associate at the same institution from Jan. 2008 to Sep. 2008. He has published over 160 articles in international journals and conference proceedings, served in the editorial boards of ASME and IEEE conferences on control systems and edited two books on control of large-scale systems (published in 2010) and LPV systems modeling, control and applications (published in 2012). His current research interests are in secure control of cyber–physical systems (and in particular, smart grids and transportation systems), coverage control of heterogeneous multi-agent systems, and learning-based control of complex distributed systems.

0093-9994 (c) 2020 IEEE. Personal use is permitted, but republication/redistribution requires IEEE permission. See http://www.ieee.org/publications_standards/publications/rights/index.html for more information.